Journal of Thermal Analysis and Calorimetry, Vol. 95 (2009) 1, 207–213

MICRO- AND NANO-THERMAL ANALYSIS APPLIED TO MULTI-LAYERED BIAXIALLY-ORIENTED POLYPROPYLENE FILMS

N. A. Gotzen[1], *G. Van Assche*[1*], *A. Ghanem*[2], *Y. Van Ingelgem*[3], *A. Hubin*[3] *and B. Van Mele*[1]

[1]Vrije Universiteit Brussel, Physical Chemistry and Polymer Science, Pleinlaan 2, 1050 Brussels, Belgium
[2]SOLVAY Research and Technology, Materials Development and Analysis Competence Centre, Rue de Ransbeek 310
1120 Brussels, Belgium
[3]Vrije Universiteit Brussel, Metallurgy, Electrochemistry and Materials Science, Pleinlaan 2, 1050 Brussels, Belgium

In this paper we compare Wollaston and silicon probes for localized thermal analysis measurements (LTA) on biaxially oriented polypropylene (BOPP) films. Up till now, no real comparison was reported in literature between the different transition temperatures measured using Wollaston and silicon probes. Using different types of probes for studying the same material proves to be very interesting. Using the Wollaston probe, the thermal properties and thickness of a 1 μm thick skin layer can be determined by through-thickness local thermal analysis measurements. The improved resolution of the silicon probes, enables the measurement of thermal properties of individual layers in a cross-sectioned film, even for layers of only 1 μm thickness. Based on the results, the silicon probes seem to be more sensitive toward the start of the melting process, since the silicon probe already penetrates at lower temperature, as compared to the Wollaston probes. This sensitivity can be exploited for studying the effect of variations in thermal history between or within samples.

Keywords: *BOPP, micro-thermal analysis, nano-thermal analysis*

Introduction

In the last decade there has been an increasing interest in the use of heated atomic force microscope (AFM) cantilever tips for various applications, such as scanning thermal microscopy [1–4], data storage [5–9], nanomanufacturing [10–13], topographical measurements [14–16], micro infra-red spectroscopy [17], room temperature chemical vapor deposition [18], localized evolved gas analysis [19] and localized thermal analysis [20–27]. Three different kinds of cantilevers with an integrated heater have emerged: the Wollaston wire [22, 28], the microfabricated wire inside polyimide [29, 30] and the micromachined doped silicon probe [31–33]. The Wollaston and the silicon probe have both been used to perform local thermal analysis (LTA) measurements. However, up till now no real comparison was made between transition temperatures measured using different probes while performing LTA measurements on the same sample. Moreover there exists a temperature gradient along the platinum-rhodium filament of the Wollaston probe, which might cause a significant temperature difference between the apex of the filament and its average temperature [34, 35]. In the case of the silicon probe, the current flows through the highly doped cantilever legs to the region at the free end where the concentration of the dopants is lower, such that it has a higher electrical resistance, inducing resistive heating at the free end above the tip. The thermal resistance across the thickness of the cantilever is small compared to the thermal resistance due to air conduction, free convection or radiation. So one can assume that the heat flows from the top of the cantilever into the substrate beneath the tip [16, 36, 37]. The heat transfer between probe and sample is complex and not yet fully understood. The possible physical mechanisms of heat transfer between probe and sample are multiple: (a) gas conduction, (b) direct heat conduction through solid-solid contact between tip and sample surface, (c) conduction through the liquid film between tip and sample surface and (d) radiative heat transfer. The predominance of these different heat transfer mechanisms depends on the sample thermal conductivity. However, modeling the differences in heat diffusion between the different probes and an evaluation of the amount of material which gets heated, was not within the scope of this work.

In this paper we compare the transition temperatures obtained by micro-thermal analysis, which uses a Wollaston probe, and by nano-thermal analysis, which uses a silicon probe, while investigating biaxially oriented polypropylene (BOPP) films. Biaxially oriented polypropylene films are extensively used in the packaging industry, as both heat sealable and non-heat sealable films. They consist of

* Author for correspondence: gvassche@vub.ac.be

1388–6150/$20.00
© 2008 Akadémiai Kiadó, Budapest
Akadémiai Kiadó, Budapest, Hungary
Springer, Dordrecht, The Netherlands

one or multiple layers having a typical total thickness of only 15–25 μm [38]. The simplest multi-layer films correspond to three-layer structures: one thick core layer of polypropylene homopolymer sandwiched between two thin (usually close to 1 μm) skin layers. Each layer has its own contribution to the properties of the film. In the standard three-layer structures, the core layer mainly provides the rigidity of the film, whereas the skin layers provide sealing and/or surface properties. Studying these systems in detail is not an easy task since it implies characterizing each individual layer. Barral *et al.* performed local thermal analysis measurements on embedded cross sections of BOPP films using micro-thermal analysis [39]. They demonstrated the melting of the core layer. In the images however, skin layers with a thickness of 1 μm or less could not be detected due to the resolution of the thermal probes. Van Assche *et al.* proved that, using through-thickness analysis, it was possible to measure accurately and rapidly the melting transition and the thickness of the skin layer with the micro-thermal analyzer without any special surface treatment or surface preparation [26]. A schematic drawing of both measurement methods is presented in Fig. 1.

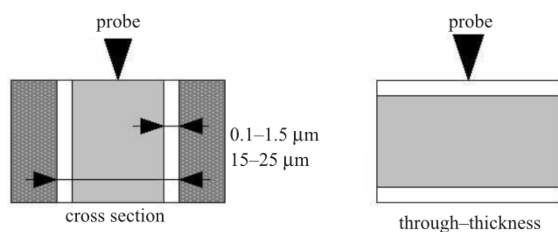

Fig. 1 Scheme of the cross-sectional measurements inside the different layers of the embedded BOPP film (left) and schematic drawing of the through-thickness analysis (right)

Experimental

Materials

Co-extruded, biaxially-oriented films with an isotactic polypropylene (iPP) core layer (about 20 μm thick) and with a skin layer of approximately 1 μm were studied. The skin layer material is a copolymer of propylene with α-olefins. All films were supplied by Solvay SA. Through-thickness analyses of the skin layers were performed on 5×5 mm^2 of film cut from a larger foil and fixed on metallic sample stubs using double-sided adhesive tape. For the nano-TA measurements on the different layers of the BOPP film ultramicrotomed cross sections were used. The film was first embedded in an epoxy matrix. After curing at 45°C for 24 h, the cross section was obtained using ultramicrotomy.

Techniques

μTA

The Micro-Thermal Analyzer μTA 2990 (TA Instruments) was operated in two modes: atomic force microscopy (AFM) and thermal analysis mode. All measurements were performed in air on a temperature controlled stage (Linkam TP 93 temperature controller with TA Instruments heat/cool stage) using a Wollaston thermal probe (Veeco). Topographic and thermal conductivity images are obtained by scanning the probe – in contact mode – over the surface while maintaining the probe at a constant temperature. Images of 100×100 μm^2 were recorded with a scanning frequency of 1 Hz using a contact force corresponding to 30 nN. The spring constant of the probe was 0.03 N m^{-1}. Local thermal analysis measurements (LTA) were performed on selected spots on the sample surface. After subtraction of a baseline recorded in air, the sensor response (in μm) of the probe is followed during a controlled fast heating (at 5 K s^{-1}). The temperature was calibrated using a two-point calibration at 30°C (on stage) and 256°C (melting of PET). For more information concerning μTA and its applications, the reader is referred to [4, 28].

Nano-TA

The nano-TA add-on (Anasys Instruments) was used in combination with a Topometrix Explorer AFM to acquire topographic images in contact mode. Using a silicon thermal probe (Anasys Instruments) it is possible to perform local thermal analysis measurements with a higher spatial resolution than obtainable with μTA. Two different probe types are available; on the one hand the AN type probe, on the other hand the GT type probe. The specifications of both probe types are given in Table 1. The GT type was used for the cross-sectional measurements, as the measurement holes resulting from the LTA's were smaller in comparison to the measurement holes obtained using the AN type. The AN type probes were used for the annealing and through-thickness measurements as they are easier in use. Images of

Table 1 Comparison between AN and GT type nano-TA probes

Probe model	GT	AN
Material	doped silicon	
Length/μm	200	300
Thickness/μm	1	2
Tip height/μm	1	3–5
Spring constant/N m^{-1}	0.1–1	0.7–2
Tip radius/nm	<40	<30
Maximum controllable temperature/°C	500	350

50×50 down to 10×10 μm^2, were recorded with a frequency of 1 Hz using a contact force of approximately 30 nN. The temperature was calibrated using a three-point calibration at 30°C (stage temperature), 61°C (melting of PCL), and 256°C (melting of PET). Local thermal analysis measurements were performed using a temperature ramp of 5 K s^{-1} from 30°C up to penetration temperature with a contact force of approximately 30 nN. The sensor signal is obtained in Volt. One can, however, calculate the sensor signal in μm, by calibrating the internal signal from the photodetector for each probe *vs*. the voltage signal which is given by the Anasys Instruments add-on.

DSC

The melting of the skin layer and core layer material was investigated in bulk by DSC using a TA Instruments Q2000 differential scanning calorimeter equipped with a refrigerated cooling system and purged with nitrogen (25 mL min^{-1}). The system was calibrated for temperature and enthalpy using the melting of indium. Non-hermetic aluminum crucibles were used in order to avoid thermal degradation. All measurements were performed at a heating rate of 10 K min^{-1}.

SEM

The different probes were observed with a JEOL JSM 6500F Scanning Electron Microscope.

Results and discussion

One has to keep in mind that the physical dimensions of the Wollaston and the silicon probe are totally different. The tip of the Wollaston probe consists in a small 2.5 μm radius platinum-rhodium filament with a radius of curvature of approximately 25 μm (Fig. 2). The silicon probe is micromachined, having a tip with a radius of curvature of approximately 30 to 50 nm, which is a little more than standard AFM probes (Figs 3 and 4). Due to the large difference in radius of curvature, the pressures exerted by the tip on the sample surface in the early stages of the measurement, before penetration due to local softening, are of a completely different order of magnitude, although the applied forces in μTA and nano-TA are comparable (30 nN). In nano-TA the pressure was calculated by using the radius of curvature and was around 10 MPa. For μTA, the contact area was calculated using the residual indents and the radius of curvature, which is a well known method [40]. In that case the calculated pressure did not exceed 200 Pa. Based on this large difference in pressure between both techniques, one

Fig. 2 SEM micrograph, showing a bottom view of the Wollaston wires and the 5 μm diameter platinum–rhodium filament used in μTA as thermal element

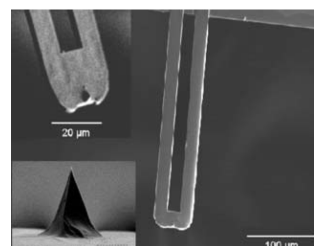

Fig. 3 SEM micrograph: general bottom view of the 300 μm long legs of the AN type nano-TA probe (right); magnified view of the 5 μm high tip (left)

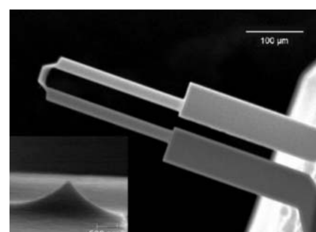

Fig. 4 SEM micrograph: general bottom view of the 200 μm long legs of the GT type nano-TA probe (right); magnified view of the 1 μm high tip (left)

can expect a different response while performing LTA measurements on the same sample.

Through-thickness analysis using μ*TA and nano-TA*

Prior to any quantitative discussion of the LTA results, it is necessary to illustrate the reproducibility of the measurements using μTA and nano-TA. Figure 5 shows through-thickness local thermal analysis experiments using μTA measured on ten different locations. The stepwise penetration proves to be very similar for all LTA's of this sample. The observed step height of the first indentation (starting around 110°C) corresponds to the thickness of the skin layer. The second indentation, starting closer to 180°C, corresponds to the sinking of the thermal probe into the iPP core layer, which melts at a more elevated temperature than the copolymer skin layer. Based on the step height of ten measurements, the skin layer thickness equals 0.9±0.1 μm. In a previous paper [26], the

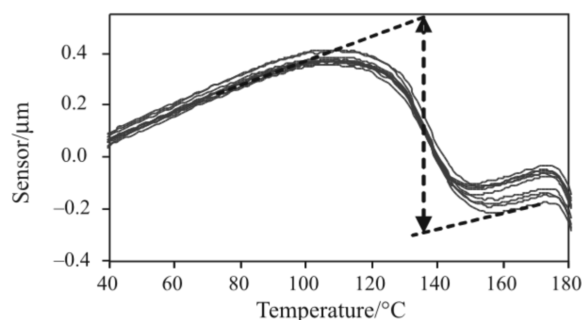

Fig. 5 Reproducibility of the local thermal analysis experiments as measured on ten different locations by through-thickness analysis of a BOPP film using μTA

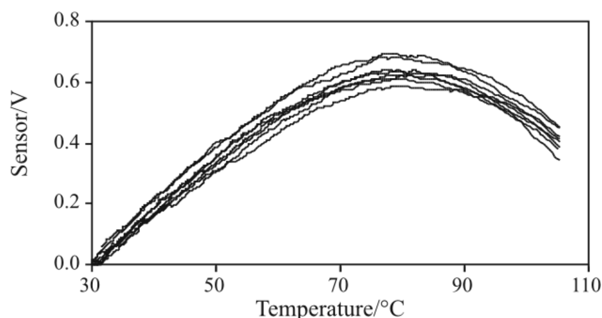

Fig. 6 Reproducibility of the local thermal analysis experiments as measured in through-thickness analysis on nine different locations using nano-TA on an annealed BOPP film

thickness obtained in μTA was shown to correspond to the one measured by TEM. The reproducibility of the local thermal analysis experiments using nano-TA is illustrated in Fig. 6. In contrast to the μTA measurements, where a complete heat-cool cycle was performed prior to withdrawing the probe tip, in nano-TA, the measurements were voluntarily stopped as soon as the first indentation started, in order to minimize the danger for tip breakage on retraction and to keep the measurement holes as small as possible. As for μTA, first a fairly straight increase is observed in the sensor signal due to the thermal expansion of the heated material and the probe. It is followed by a downward curving caused by the penetration of the probe tip into the material. The maximum at 78°C is taken as the transition temperature. These results indicate that the penetration as observed in nano-TA, starts at a lower temperature in comparison with μTA. Due to their difference in physical dimensions, μTA and nano-TA probe different thermal effects. To support this statement, μTA and nano-TA experiments were performed on BOPP films annealed at 60°C for 24 h. The annealing of the skin layer material was first studied in bulk using DSC (Fig. 7). The melting of the skin layer material starts at 51°C for the non-annealed sample and is shifted to 64°C due to the perfectioning of the crystal lamellae upon annealing.

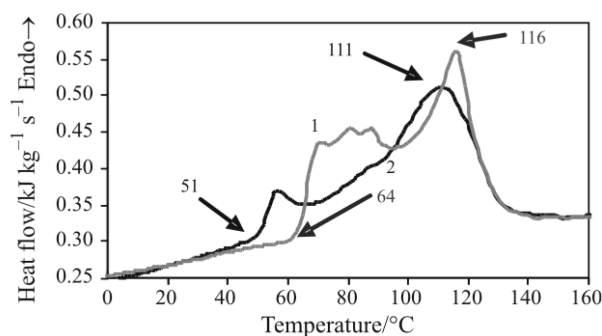

Fig. 7 Melting of a bulk sample of the skin layer material 1 – annealed at 60°C for 24 h and 2 – non-annealed, measured with DSC. The onset of the melting is shifted to higher temperatures due to the perfectioning of the crystal lamellae upon annealing

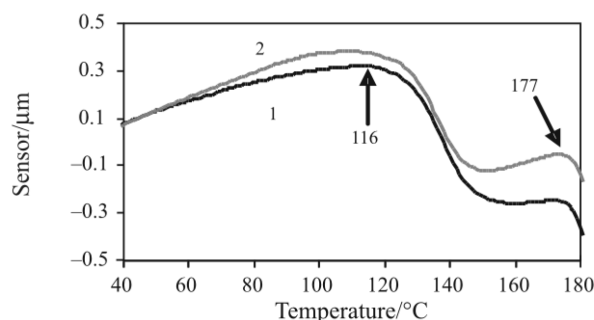

Fig. 8 Local thermal analysis measurements for 1 – non-annealed and 2 – annealed BOPP film, measured by through-thickness analysis with μTA

The largest fraction of the crystals melts at 111°C in the case of the non-annealed and 116°C in the case of the annealed samples. The effect of annealing as observed by μTA in a through-thickness measurement is illustrated in Fig. 8. This graph shows the average of five LTA's for non-annealed and annealed samples, measured in different areas with the same thermal probe. In the non-annealed sample, the sensor signal shows a smaller increase before the main penetration around 116°C. This is due to a slow gradual penetration of the probe into the material. In the annealed samples no slow penetration is observed until the same major step at 116°C. Thus the gradual melting of the material between the onset and the main peak of the melting range leads to a gradual penetration of the μTA probe. Nevertheless, the major step is only observed when the majority of the crystals has molten and is quasi-independent of the annealing, which is in good agreement with Fig. 7. In the case of the nano-TA experiments (Fig.9), the sensor maximum is observed 6°C earlier for the non-annealed sample in comparison to the annealed one, with a maximum at 72 and 78°C, respectively. This is well below the main penetration observed in μTA and demonstrates that nano-TA is truly sensitive to the effect of the an-

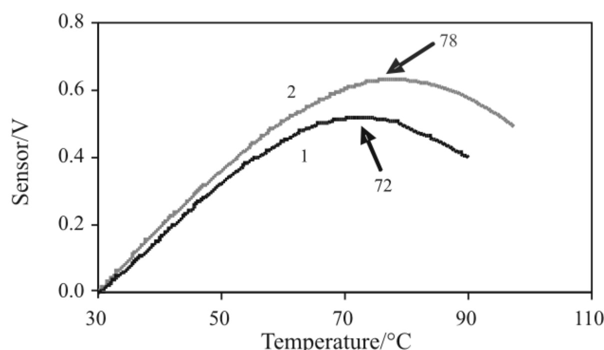

Fig. 9 Local thermal analysis measurements for 1 – non-annealed and 2 – annealed BOPP film, measured by through-thickness analysis with nano-TA

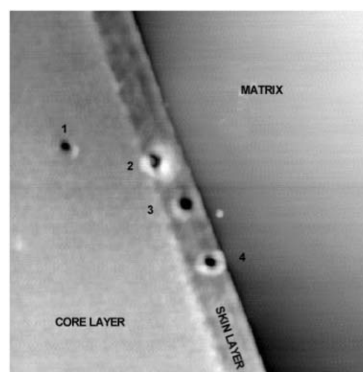

Fig. 10 10×10 μm^2 image of a three-layer BOPP film embedded in an epoxy resin showing the 1 μm skin layer (middle), the core layer (left) and the epoxy resin (right) in which the film is embedded. Four holes in the BOPP core and skin layer resulting from previous LTA measurements using nano-TA GT type probe can be seen

nealing procedure on the onset of the melting. Hence, nano-TA seems to be sensitive to smaller changes in the start of the melting process; probably a smaller fraction needs to melt for the probe to penetrate due to the very high aspect ratio of the probe in comparison to the μTA Wollaston probe. This indicates the need for narrow-melting range materials for the temperature calibration. In contrast, μTA is mainly probing the end of the melting process.

Thus, both μTA and nano-TA show differences between the annealed and the non-annealed films. However in μTA, the difference is very small since the temperature of the main penetration in the skin layer is not significantly influenced. In nano-TA however, the temperature of the maximum of the sensor signal is significantly increased due to the annealing procedure.

Cross section analysis using nano-TA

The higher spatial resolution of the nano-TA probes enables one to study individual layers in cross sections of multilayered films. Figure 10 shows a 10×10 μm^2 topographic image, obtained in contact mode, in which the 0.9 μm skin layer can be seen. Inside the different layers, the holes resulting from LTA measurements using nano-TA can clearly be observed. In the LTA curves shown in Fig. 11, initially a straight rise in the sensor signal is observed for all materials due to the thermal expansion of the heated material and the probe, followed by a (gradual) downward curving caused by the penetration of the probe tip into the material. To avoid tip breakage upon retraction, the tip is retracted as soon as the penetration is observed. The maximum is taken as the transition temperature. For the iPP core layer the melting is observed around 147°C and for the copolymer skin layer around 78°C. For the epoxy resin, the penetration of the probe tip due to the softening at the glass transition is observed around 66°C. Comparison with DSC experiments on the individual skin and core layer materials, indicates again that in nano-TA the transition

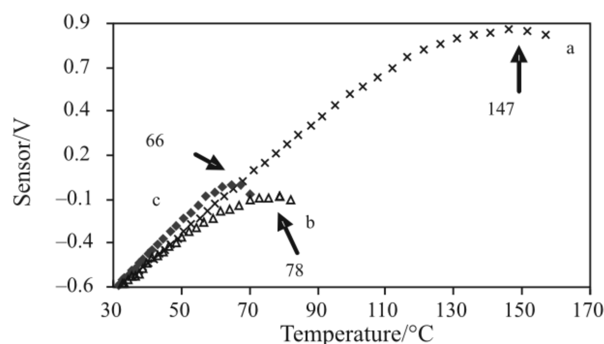

Fig. 11 Local thermal analysis measurements, performed using the GT type probe, inside a – core layer, b – skin layer and c – epoxy matrix, measured on a cross section with nano-TA

is observed when only a limited fraction of the material has molten (neither of these two materials were used as calibrants for nano-TA) (Fig. 12). It should be noted here that only a qualitative comparison can be made with the DSC results, as these are performed on bulk samples instead of films with a preferential in-plane orientation of the chains induced by drawing.

These local thermal analysis results clearly distinguish between the different materials. Moreover the layers can not only be identified, but the effects of processing (e.g. annealing) on the individual layers can be studied directly, as was illustrated in the previous section. However, this is only the case on the condition that the material properties are unaffected by the embedding and cross sectioning procedure required to obtain cross sections.

The discrepancy in the melting temperatures of the iPP core layer as detected by μTA (177°C) and nano-TA (147°C) in comparison to the DSC value on the bulk material (160°C) is due to mainly two reasons. In μTA, the transition temperature was determined by a through-thickness measurement, whereas, in the case of

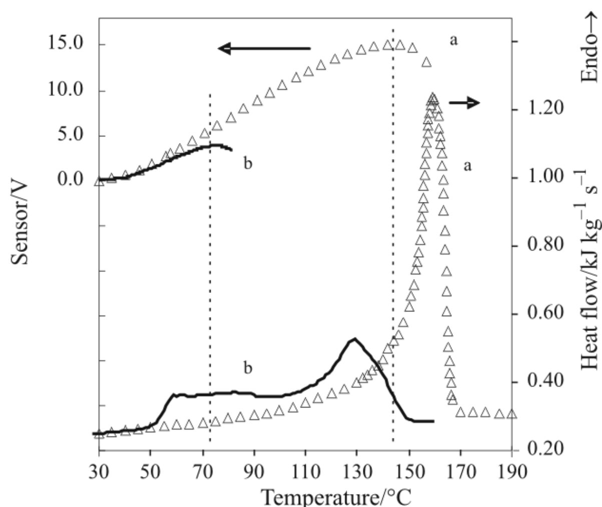

Fig. 12 Local thermal analysis measurements, performed using the AN type silicon probe, inside a – core layer and b – skin layer measured on a cross section with nano-TA compared to the melting of the bulk materials measured using DSC

nano-TA, the melting of the core layer is detected in a cross sectional measurement. This means that, in μTA, the probe first has to indent through the skin layer in order to heat up the underlying core layer material, which usually causes a transition at a higher temperature in comparison to DSC. While in nano-TA the measurement is performed directly on the iPP core layer. Moreover, as was the case for the measurements on the skin layer material, the melting is detected in the early stages of the melting process. This due to the large contact pressure under the nano-TA tip (10 MPa) in comparison to μTA (200 Pa) and the very small sample size of the heated zone under the tip.

Despite the fact that the skin layer materials in the through-thickness and the cross sectional measurements are different, their melting onset temperature, as measured using DSC, is in both cases 51°C (Figs 7 and 12). The transition temperatures obtained using nano-TA are 72 and 73°C, respectively (Figs 9 and 12). Both measurements were performed with the same probe type (AN), but with a different probe and a different calibration file. This is a strong evidence of the reproducibility of the calibration and the stated sensitivity of nano-TA to the initial stages of the melting process as detected by DSC.

Conclusions

The improved resolution of the nano-TA enables us to perform local thermal analysis measurements inside the different layers on cross sections of multi-layered films, even for layers of less than 1 μm thickness. This is a major amelioration in comparison with μTA, offering new opportunities for the study of layered films and the study of multiphase materials in general. The major advantage of μTA in comparison with nano-TA is the ease by which the thickness information is obtained when performing a through-thickness measurement. The results illustrate that μTA is more sensitive to the end of the melting process, while nano-TA probes the early stages of the melting process. Using both types of probes will improve the comparative analysis of samples having differences in the shape of their melting transition either due to the intrinsic material properties or their thermal history. This opens prospects for the study of local differences in melting behavior in cross sectioned bulk samples, e.g., injection-molded parts, since this would allow us to obtain information on the local thermal history of the material.

Acknowledgements

The Research Foundation Flanders (FWO-Vlaanderen) is kindly acknowledged for supporting this research by a Ph.D. and a post-doctoral research grant.

References

1 M. Nonnenmacher and H. K. Wickramasinghe, Appl. Phys. Lett., 61 (1992) 168.
2 A. Hammiche, H. M. Pollock, M. Song and D. J. Hourston, Meas. Sci. Technol., 7 (1996) 142.
3 A. Hammiche, D. Price, E. Dupas, G. Mills, A. Kulik, M. Reading, J. Weaver and H. Pollock, J. Microsc. – Oxford, 199 (2000) 180.
4 M. Song, D. Hourston, D. Grandy and M. Reading, J. Appl. Polym. Sci., 81 (2001) 2136.
5 M. I. Lutwyche, M. Despont, U. Drechsler, U. Durig, W. Haberle, H. Rothuizen, R. Stutz, R. Widmer, G. K. Binnig and P. Vettiger, Appl. Phys. Lett., 77 (2000) 3299.
6 P. Vettiger, M. Despont, U. Drechsler, U. Durig, W. Haberle, M. I. Lutwyche, H. E. Rothuizen, R. Stutz, R. Widmer and G. K. Binnig, IBM J. Res. Dev., 44 (2000) 323.
7 U. Durig, G. Cross, M. Despont, U. Drechsler, W. Haberle, M. I. Lutwyche, H. Rothuizen, R. Stutz, R. Widmer, P. Vettiger, G. K. Binnig, W. P. King and K. E. Goodson, Tribol. Lett., 9 (2000) 25.
8 W. P. King, T. W. Kenny, K. E. Goodson, G. Cross, M. Despont, U. Durig, H. Rothuizen, G. K. Binnig and P. Vettiger, Appl. Phys. Lett., 78 (2001) 1300.
9 W. P. King and K. E. Goodson, J. Heat Trans.-T. ASME, 124 (2002) 597.
10 P. E. Sheehan, L. J. Whitman, W. P. King and B. A. Nelson, Appl. Phys. Lett., 85 (2004) 1589.
11 B. A. Nelson, W. P. King, A. R. Laracuente, P. E. Sheehan and L. J. Whitman, Appl. Phys. Lett., 88 (2006) 033104.
12 M. Yang, P. E. Sheehan, W. P. King and L. J. Whitman, J. Am. Chem. Soc., 128 (2006) 6774.

13 S. Bakbak, P. J. Leech, B. E. Carson, S. Saxena, W. P. King and U. H. F. Bunz, Macromolecules, 39 (2006) MA0615912.
14 K. J. Kim, K. Park, J. Lee, Z. M. Zhang and W. P. King, Sens. Actuators, A-Phys., 136 (2007) 95.
15 W. P. King, T. W. Kenny and K. E. Goodson, Appl. Phys. Lett., 85 (2004) 2086.
16 W. P. King, J. Micromech. Microeng., 15 (2005) 2441.
17 M. Reading, D. Grandy, A. Hammiche, L. Bozec and H. M. Pollock, Vib. Spectrosc., 29 (2002) 257.
18 E. O. Sunden, T. L. Wright, J. Lee, W. P. King and S. Graham, Appl. Phys. Lett., 88 (2006) 033107.
19 D. M. Price, M. Reading, T. J. Lever, A. Hammiche and H. M. Pollock, Thermochim. Acta, 367368 (2001) 195.
20 A. Hammiche, M. Reading, H. M. Pollock, M. Song and D. J. Hourston, Rev. Sci. Instrum., 67 (1996) 4268.
21 D. M. Price, M. Reading, A. Hammiche, H. M. Pollock and M. G. Branch, Thermochim. Acta, 332 (1999) 143.
22 D. M. Price, M. Reading, A. Hammiche and H. M. Pollock, J. Therm. Anal. Cal., 60 (2000) 723.
23 P. G. Royall, D. Q. M. Craig, D. M. Price, M. Reading and T. J. Lever, Int. J. Pharm., 192 (1999) 97.
24 D. B. Grandy, D. J. Hourston, D. M. Price, M. Reading, G. G. Silva, M. Song and P. A. Sykes, Macromolecules, 33 (2000) 9348.
25 G. Van Assche and B. Van Mele, Polymer, 43 (2002) 4605.
26 G. Van Assche, A. Ghanem, O. Lhost and B. Van Mele, Polymer, 46 (2005) 7132.
27 B. A. Nelson and W. P. King, Rev. Sci. Instrum., 78 (2007) 023702.
28 H. Pollock and A. Hammiche, J. Phys. D Appl. Phys., 34 (2001) R23.
29 M. H. Li, J. J. Wu and Y. B. Gianchandani, J. Microelectromech. Syst., 10 (2001) 3.
30 J. H. Lee and Y. B. Gianchandani, Rev. Sci. Instrum., 75 (2004) 1222.
31 L. Harding, M. Reading, C. Duncan, K. Kjoller and N. A. Gotzen, Innov. Pharm. Tech., 21 (2006) 78.
32 W. P. King, S. Saxena, B. A. Nelson, B. L. Weeks and R. Pitchimani, Nano Lett., 6 (2006) 2145.
33 T. Gray, J. Killgore, J. D. Luo, A. K. Y. Jen and R. M. Overney, Nanotechnology, 18 (2007) 044009.
34 S. Gomes, N. Trannoy and P. Grossel, Meas. Sci. Technol., 10 (1999) 805.
35 S. Gomes, N. Trannoy, P. Grossel, F. Depasse, C. Bainier and D. Charraut, Int. J. Therm. Sci., 40 (2001) 949.
36 N. D. Masters, W. J. Ye and W. P. King, Phys. Fluids, 17 (2005) 100615.
37 J. Lee, T. L. Wright, M. R. Abel, E. O. Sunden, A. Marchenkov, S. Graham and W. P. King, J. Appl. Phys., 101 (2007) 014906.
38 G. Agrawal and S. Mannan, Chem. Eng. World, 30 (1995) 33.
39 M. Abad, A. Ares, L. Barral, J. Cano, F. Diez, J. Lopez and C. Ramirez, J. Appl. Polym. Sci., 85 (2002) 1553.
40 F. Yang, E. Wornyo, K. Gall and W. P. King, Nanotechnology, 18 (2007) 285302.

Received: December 7, 2007
Accepted: April 23, 2008
OnlineFirst: August 15, 2008

DOI: 10.1007/s10973-007-8931-9